Journal of Solid State Chemistry 182 (2009) 3067–3070

Contents lists available at ScienceDirect

Journal of Solid State Chemistry

journal homepage: www.elsevier.com/locate/jssc

A 3D porous indium(III) coordination polymer involving *in-situ* ligand synthesis

Zheng-Bo Han *, Yong-Juan Song, Jian-Wei Ji, Wei Zhang, Guang-Xi Han

College of Chemistry, Liaoning University, Shenyang 110036, PR China

ARTICLE INFO

Article history:
Received 26 February 2009
Received in revised form
17 August 2009
Accepted 22 August 2009
Available online 29 August 2009

Keywords:
Coordination polymer
In(III)
In-situ ligand synthesis
Porous metal–organic framework

ABSTRACT

The hydrothermal reaction of In^{3+} and 1,2,4-benzenetricarboxylic acid with the presence of piperazine leads to the generation of a novel 3D porous coordination polymer, $[H_3O][In_2(btc)(bdc)(OH)_2]\cdot 5.5H_2O$ (**1**), (btc=1,2,4-benzenetricarboxylate, bdc=1,4-benzenedicarboxylate). Compound **1** crystallizes in orthorhombic space group *Pbca* with $a=16.216(7)$ Å, $b=13.437(6)$ Å, $c=31.277(14)$ Å, and $Z=8$. It is interesting to find that the *in-situ* decarboxylation reaction of 1,2,4-benzenetricarboxylate (btc) partially transformed into 1,4-benzenedicarboxylate (bdc) occurs. The 16 indium(III) centers were linked by four btc, four bdc and two μ_2-OH ligands to form a box-girder. The adjacent box-girders are further connected by the bdc and btc ligands to generate a novel porous metal–organic framework containing nanotubular open channel with a cross-section of approximately 11.5×11.3 Å^2. The micropores are occupied by lattice water molecules, and the solvent-accessible volume of the unit cell was estimated to be 3658.6 Å^3, which is approximately 53.7% of the unit-cell volume (6815.4 Å^3).

1. Introduction

In recent years, increasing research interest has been drawn to explore the porous metal–organic frameworks (MOFs) for potential applications in ion-exchange, gas storage, magnetism and heterogeneous catalysis [1–10]. The porous MOFs have many advantages in that they can provide not only light materials with high porosity but also desirable regular networks. Compared with the inorganic porous materials such as zeolites and metal phosphates, metal–organic coordination polymers can be designed and constructed to generate cavities or channels of various sizes and shapes by controlling the architecture and function of the organic linkers [11,12].

Various multi-carboxylate ligands, for example, 1,2,4,5-benzenetetracarboxylate (btec), 1,4-benzenedicarboxylate (bdc) and 1,3,5-benzenetricarboxylate (1,3,5-btc) [13–17], have been used in the assembly of robust MOFs. However, in contrast to the above multi-carboxylate ligands, 1,2,4-btc is rarely employed in the construction of metal–organic coordination polymers [18,19]. It may be argued that, due to steric reasons, btec, bdc and 1,3,5-btc ligands have highly symmetrical geometries, While 1,2,4-btc ligand has an asymmetric geometry and possesses three inequally spaced carboxylate groups, consequently, it is difficult to coordinate to metal ions. In this paper, we report on the synthesis, structure and photoluminescent properties of $[H_3O][In_2(btc)(bdc)(OH)_2]\cdot 5.5H_2O$ (**1**). Interestingly, *in-situ* decarboxylation reaction occurred and btc ligand was partially transformed into bdc ligand (Scheme 1) which is different from the previously reported *in-situ* ligand reactions [20–29], such as ligand oxidative coupling, hydrolysis, cleavage of C–S or C–C bonds, and hydroxylation of aromatic groups and cycloaddition of organonitriles with ammonia.

2. Experimental section

2.1. Materials and methods

All chemicals and solvents employed were commercially available and used as received without further purification. The C, H, and N microanalysis was carried out with Perkin-Elmer 240 elemental analyzer. The FT-IR spectra were recorded from KBr pellets in the 4000–400 cm^{-1} range on a Nicolet 5DX spectrometer. X-ray power diffraction (XRPD) was recorded on a Bruker AXS D8 advanced automated diffractometer with Cu*K*α radiation. Thermal analysis (TGA) was performed on a NETZSCH TG 209 instrument under nitrogen with a heating rate of 10 °C min^{-1}. The emission spectra were recorded on a Perkin-Elmer LS50B fluorescence spectrophotometer.

2.2. Synthesis of $[H_3O][In_2(btc)(bdc)(OH)_2]\cdot 5.5H_2O$ (**1**)

A mixture of $In(NO_3)_3\cdot 5H_2O$ (0.195 g, 0.5 mmol), 1,2,4-H_3btc (0.32 g, 1.5 mmol), piperazine (0.388 g, 2 mmol) and H_2O (10 ml) was mixed in a 23 mL Teflon reactor, which was heated at 443 K

* Corresponding author. Fax: +86 24 62202380.
E-mail address: ceshzb@lnu.edu.cn (Z.-B. Han).

0022-4596/$ - see front matter Crown Copyright © 2009 Published by Elsevier Inc. All rights reserved.
doi:10.1016/j.jssc.2009.08.024

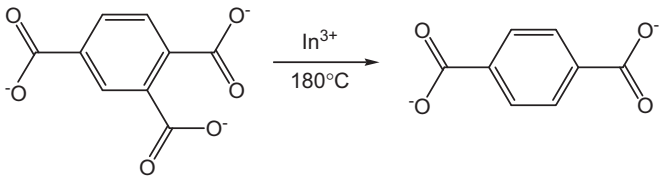

Scheme 1

Table 1
Crystallographic data for **1**.

Empirical formula	$C_{17}H_{23}In_2O_{18.5}$
Formula weight	752.99
Wavelength (Å)	0.71073
Crystal system	Orthorhombic
Space group	*Pbca*
Unit cell dimensions	
a (Å)	13.502(2)
b (Å)	15.465(2)
c (Å)	32.416(4)
V (Å^3)	6768.2(17)
Z	8
Dc (g cm^{-3})	1.478
μ (mm^{-1})	1.427
F(000)	2968
Crystal size/mm	0.37 × 0.32 × 0.23
Range for data collection (deg)	2.63–25.00
Reflections collected	6905
Independent reflections	5677
Max, min transmission	0.8318 and 0.6211
T (K)	293(2)
Goodness-of-fit on F^2	1.064
Data/restraints/parameters	5677/0/355
Final *R* indices [$I > 2\sigma(I)$][a]	R_1=0.0569, wR_2=0.1540
R indices (all data)	R_1=0.0828, wR_2=0.1733
Largest diff. peak and hole (e Å^{-3})	1.688 and −1.026
CCDC reference number	714332

for 3 days and then cooled to room temperature at a rate of 10 K h^{-1}. Orange–yellow block crystals of **1** were obtained in 78% yield after being washed with distilled water and dried in air. Anal. Calcd. for $C_{17}H_{23}In_2O_{18.5}$ (**1**): C, 27.12; H, 3.08. Found: C, 27.33; H, 2.92. IR (KBr, cm^{-1}): 3455(s), 1618(s), 1488(m), 1383(s), 1311(w), 1024(w), 588(m).

2.3. X-ray crystallography

Crystallographic data of **1** were collected at room temperature with a Bruker P4 diffractometer with Mo*K*α radiation (α=0.71073 Å) and graphite monochromator using the ω-scan mode. The structure was solved by direct method and refined on F^2 by full-matrix least squares using SHELXTL [30]. All non-hydrogen atoms were treated anisotropically. The positions of the hydrogen atoms were generated geometrically. CCDC reference number 714332. Crystallographic data and experimental details for structural analysis are summarized in Table 1. Copy of the data can be obtained free of charge on application to CCDC, 12 Union Road, Cambridge CB2 1EZ, UK [Fax: +44 1223 336 033; E-mail: deposit@ccdc.cam.ac.uk].

3. Results and discussion

Structure of $[H_3O][In_2(btc)(bdc)(OH)_2]\cdot 5.5H_2O$ **(1)** Compound **1** exhibits a 3D porous framework in which the asymmetric unit

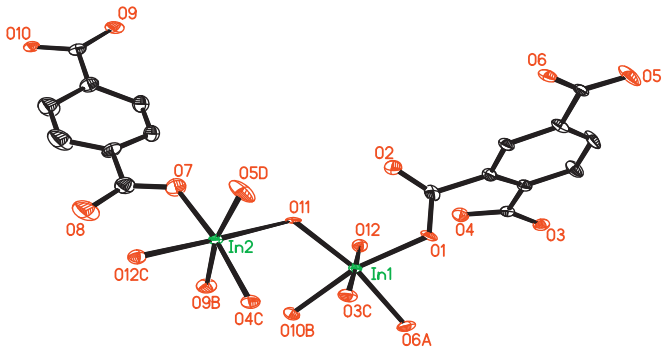

Fig. 1. Coordination environments of two Indium(III) ions, including btc and bdc in **1**. H atoms and water molecules were omitted for clarity. Selected bonds lengths: In(1)–O(6A) 2.068(6), In(1)–O(10B) 2.118(6), In(1)–O(11) 2.118(5), In(1)–O(1) 2.142(6), In(1)–O(12) 2.247(6), In(1)–O(3C) 2.328(6), In(2)–O(7) 2.025(6), In(2)–O(4C) 2.056(6), In(2)–O(5D) 2.061(6), In(2)–O(9B) 2.065(6), In(2)–O(11) 2.338(6), In(2)–O(12C) 2.364(6) Å. Selected bond angles (o): O(11)–In(1)–O(1) 113.1(2), O(11)–In(1)–O(12) 98.7(2), O(1)–In(1)–O(12) 91.5(2), O(7)–In(2)–O(11) 92.7(2). Symmetry code: (A) $x+1/2,y,-z+1/2$; (B) $x+1/2,-y+1/2,-z+1$; (C) $-x+1/2,y+1/2,z$; (D) $-x,y+1/2,-z+1/2$.

contains two In(III) ions, one btc, one bdc, two hydroxyl groups and six and a half lattice water molecules. Fig. 1 shows the coordination environment of two independent In(III) ions. Each In(1) is coordinated by two hydroxyl oxygen atoms (O11 and O12) and four carboxylate oxygen atoms from two individual btc ligands and two individual bdc ligands to form a slightly distorted octahedronal coordination geometry. Each In(2) is also coordinated by two hydroxyl oxygen atoms (O11 and O12) and four carboxylate oxygen atoms from one bdc ligand and three individual btc ligands to form a slightly distorted octahedronal coordination geometry. The In–O bond distances ranging from 2.025(6) to 2.247(6) are in the normal range [31,32]. Three carboxylate groups of the btc ligands are all depronated, one of them coordinates to an In(III) atom in a monodentate mode, while the other two link two In(III) centers in a bidentate bridging mode. Each 1,4-bdc ligand connects three indium centers, with one monodentate carboxylic group connecting one indium center and the other carboxylic group bridging two indium centers. As shown in Fig. 2, the 16 In(III) centers were linked by four bdc ligands, four btc ligands and two μ_2-OH groups to form a box-girder. The adjacent box-girders are further connected by the bdc and btc ligands to generate a novel porous metal–organic framework containing nanotubular open channels (Fig. 3a). Fig. 3b shows the framework structure surrounding a single nanotubular channel along the crystallographic *b* axis with a cross-section of approximately 11.5 × 11.3 Å^2. Interestingly, there exist 1D zigzag In–OH–In chains running along the *b* axis with the intrachain In–In distances of 3.725(1) and 3.623(2) Å (Fig. 3c). The lattice water molecules are present in the channels of the 3D framework. After omitting the lattice water molecules, the solvent-accessible volume of the unit cell was estimated (PLATON program [33]) to be 3658.6 Å^3, which is approximately 53.7% of the unit-cell volume (6815.4 Å^3).

Bond valence sum (BVS) calculations [34] confirm that all indium centers have an oxidation state of +3 and O11 and O12 give the oxidation state of 1.1 and 1.2, respectively, which further support that the O11 and O12 atoms are hydroxyl oxygen atoms.

It is interesting to note the occurrence of decarboxylation that btc was partially transformed into bdc under the hydrothermal conditions. Decarboxylation reactions catalyzed by enzyme [35] and transition metal [36] have been extensively studied over the past century due to the importance of the carboxylation/decarboxylation reactions in the carbon cycle. However, to the best of our knowledge, indium-triggered decarboxylation reaction

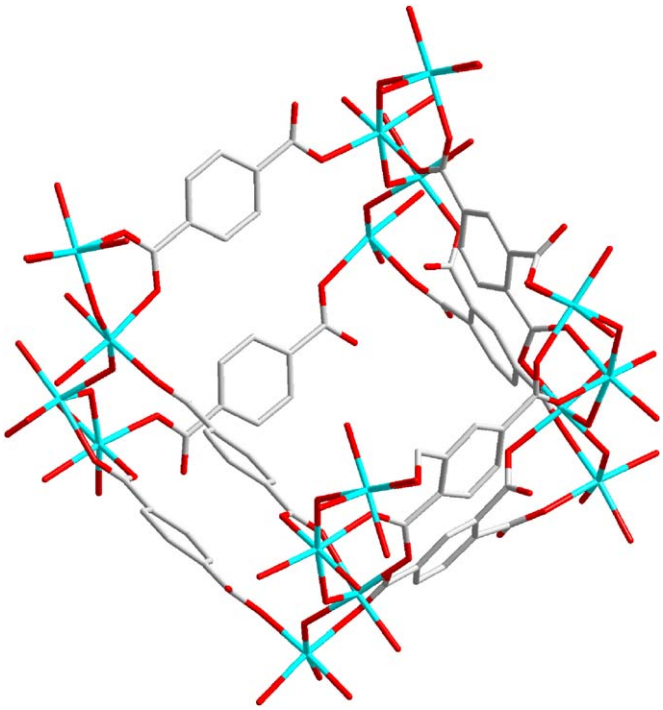

Fig. 2. A $[In_{16}(btc)_4(bdc)_4(OH)_8]$ box-girder.

has been rare reported [37]. In contrast, no decarboxylation occurred in the reactions of transition metal (Co, Na, Cd) ions with btc ligands under similar conditions [38–40]. Compared with the previously reported *in-situ* decarboxylation in the copper(II) and lanthanide complexes, 1,2,3-benzenetricarboxylic acid was transformed into 1,3-benzenedicarboxylic acid [41], 3,4-pyridinedicarboxylic acid was partially transformed into isonicotinic acid [42] and 2,3-pyridinedicarboxylic acid was transformed into nicotinic acid [43], we can deduce that that the metal atomic radius and the steric hindrance of the organic ligands may have important effect on the decarboxylation reaction.

3.1. IR spectra, TGA and XRPD patterns

The IR spectra of compound **1** show the absorption peaks in the region of 3455 cm^{-1} may be assigned to the stretching vibrations of the lattice water molecules. The bands at 1618(s), and 1488(m), 1383(s) cm^{-1} are due to the asymmetric and symmetric stretching vibrations of the carboxylate groups, respectively. The absence of the characteristic bands at 1720–1690 cm^{-1} attributed to the protonated carboxylate groups indicates that all the H_3btc and H_2bdc are deprotonated [44]. The TGA curve of **1** (Fig. 1S) shows two steps of weight loss. The first weight loss of 15.32% below 190 °C, corresponding to the loss of the lattice water molecules (calculated 15.54%). The second one from 250 to 820 °C (found 49.68%, calculated 49.96%) indicates the decomposition of the organic ligands, leading to the generation of In_2O_3. The experimental and simulated X-ray XRPD patterns of **1** were shown in Fig. 4, their peaks are in good agreement with each other, substantiating the phase purity of the as-synthesized products. The difference in reflection intensity is probably caused by the preferred orientation effect in the powder sample. The absence of some reflections might be a result of their relatively low intensity. This framework is stable up to 190 °C, which is confirmed by the XRPD patterns after heating at 190 °C for 14 h (Fig. 4).

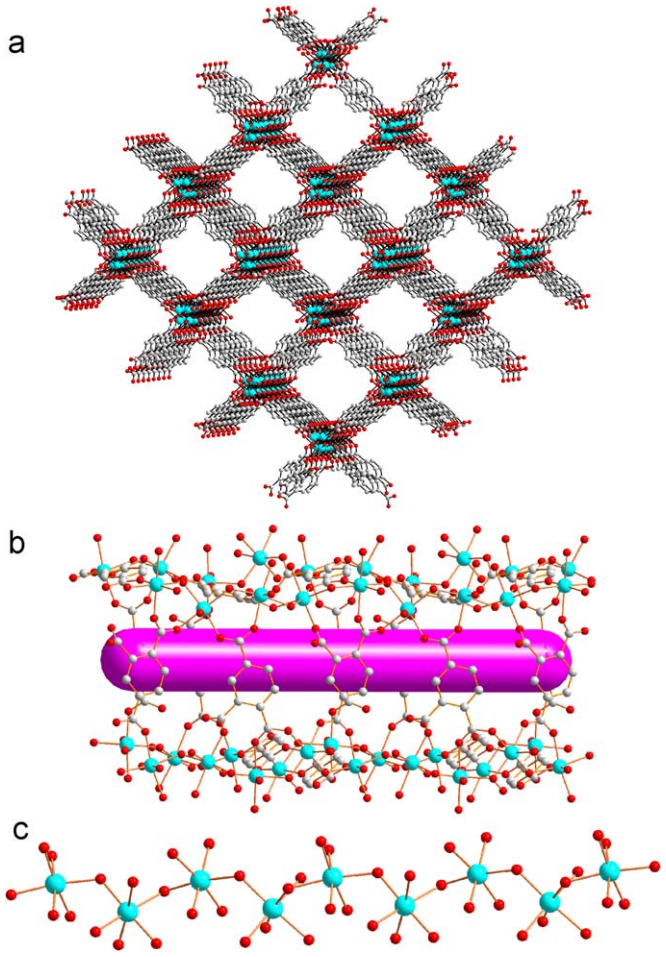

Fig. 3. (a) 3D framework of **1**, showing the nanotubular channels along the *a* axis (the lattice water molecules are omitted for clarity). (b) View of the open channel along the *b* axis (the purple bar represents free space inside the open channel). (c) View of the In–OH–In chain along the b axis.

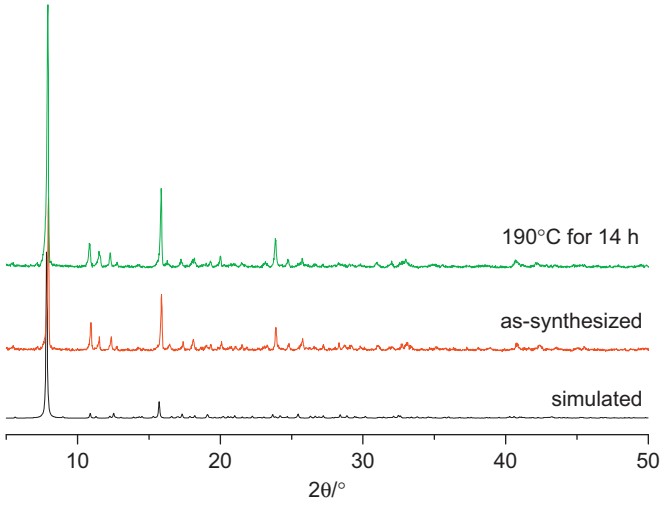

Fig. 4. The simulated, experimental and after heating XRPD patterns for **1**.

3.2. Photoluminescent properties

Photoluminescent spectra of **1** are shown in Fig. 5. Strong fluorescent emission band at 447 nm (*ex*=300 nm) is observed in

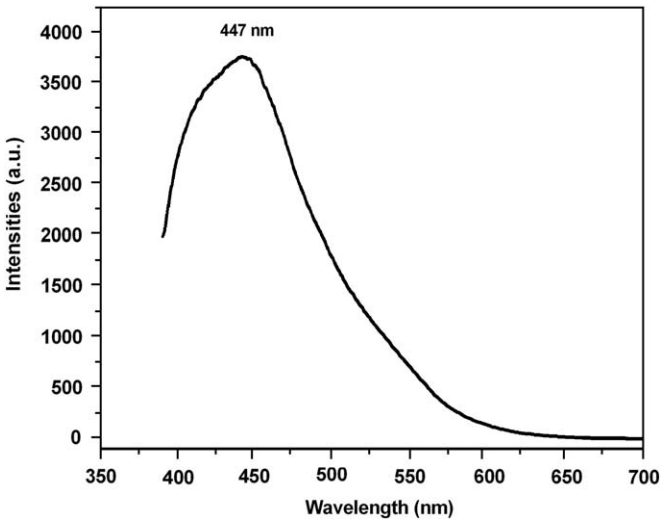

Fig. 5. Solid state photoluminescent spectra of **1**.

the solid state at room temperature. The photoluminescent properties of hybrid inorganic–organic compounds are usually assigned to ligand-to-metal charge transfers (LMCT), metal-to-ligand charge transfers (MLCT), metal-centered transitions, or interligand $\pi-\pi^*$ transitions. Taking into account the emission of free bdc or btc ligands at *ca.* 420 nm [45,46], the emission of compound **1** may be originated from the ligand-to-metal charge transfer (LMCT). This observation indicates that compound **1** may be an excellent candidate for potential photoactive materials.

4. Conclusions

In summary, the In(III) porous MOF, $[H_3O][In_2(btc)(bdc)(OH)_2]\cdot 5.5H_2O$, has been synthesized by hydrothermal technique. Structural analysis indicates that **1** features a 3D porous MOF structure with infinite In–OH–In chains. The lattice water molecules fill in the channels. This framework is stable up to 190 °C, which is confirmed by the XRPD patterns after heating at 190 °C. Interestingly, the *in-situ* C–C bond cleavage occurred and btc ligand was partially transformed into bdc ligand. The successful synthesis of **1** opens the field of synthetic chemistry in metal 1,2,4-benzenetricarboxylate and it is believed that more In(III) multicarboxylate with interesting structural architectures will be continuously synthesized under suitable synthetic conditions.

Supplementary information available

TGA curve and X-ray crystallographic file of **1**.

Acknowledgments

This work was granted financial support from National Natural Science Fundation of China (20871063).

Appendix A. Supplementary material

Supplementary data associated with this article can be found in the online version at doi:10.1016/j.jssc.2009.08.024.

References

[1] S.L. James, Chem. Soc. Rev. 32 (2003) 276.
[2] D. Bradshaw, J.B. Claridge, E.J. Cussen, T.J. Prior, M.J. Rosseinsky, Acc. Chem. Res. 38 (2005) 273.
[3] N.W. Ockwig, O. Delgado-Friedrichs, M. O'Keeffe, O.M. Yaghi, Acc. Chem. Res. 38 (2005) 176.
[4] M. Eddaoudi, D.B. Moler, H.L. Li, B.L. Chen, T.M. Reineke, M. O'Keeffe, O.M. Yaghi, Acc. Chem. Res. 34 (2001) 319.
[5] S.R. Batten, R. Robson, Angew. Chem. Int. Ed. 37 (1998) 1460.
[6] B. Moulton, M.J. Zaworotko, Chem. Rev. 101 (2001) 1629.
[7] X.B. Zhao, B. Xiao, A.J. Fletcher, K.M. Thomas, D. Bradshaw, M.J. Rosseinsky, Science 306 (2004) 1012.
[8] C.A. Bauer, T.V. Timofeeva, T.B. Settersten, B.D. Patterson, V.H. Liu, B.A. Simmons, M.D. Allendorf, J. Am. Chem. Soc. 129 (2007) 7136.
[9] N.L. Rosi, J. Eckert, M. Eddaoudi, D.T. Vodak, J. Kim, M. O'Keeffe, O.M. Yaghi, Science 300 (2002) 1127.
[10] J.Y. Lee, L. Pan, S.P. Kelly, J. Jagiello, T.J. Emge, J. Li, Adv. Mater. 17 (2005) 2703.
[11] H.J. Choi, M.P. Suh, J. Am. Chem. Soc. 120 (1998) 10622.
[12] O.R. Evans, W. Lin, Acc. Chem. Res. 35 (2002) 511.
[13] K. Barthelet, D. Riou, G. Férey, Chem. Commun. (2002) 1492.
[14] M. Eddaoudi, H. Li, O.M. Yaghi, J. Am. Chem. Soc. 122 (2000) 1391.
[15] T.M. Reineke, M. Eddaoudi, M. O'Keeffe, O.M. Yaghi, Angew. Chem. Int. Ed. Engl. 38 (1999) 2590.
[16] D. Cheng, M.A. Khan, R.P. Houser, Inorg. Chem. 40 (2001) 6858.
[17] H. Kumagai, C.J. Kepert, M. Kurmoo, Inorg. Chem. 41 (2002) 3410.
[18] L. Wang, Z. Shi, G.H. Li, Y. Fan, W.S. Fu, S.H. Feng, Solid State Sci. 6 (2004) 85.
[19] Z.L. Lü, W. Chen, J.Q. Xu, L.J. Zhang, C.L. Pan, T.G. Wang, Inorg. Chem. Commun. 6 (2003) 244.
[20] J. Tao, Y. Zhang, M.L. Tong, X.M. Chen, T. Yuen, C.L. Lin, X.Y. Huang, J. Li, Chem. Commun. (2002) 1342.
[21] O.R. Evans, W. Lin, Cryst. Growth & Des.1 (2001) 9.
[22] X.M. Zhang, M.L. Tong, X.M. Chen, Angew. Chem. Int. Ed. 41 (2002) 1029.
[23] M. Zhang, R.Q. Fang, H.S. Wu, J. Am. Chem. Soc. 127 (2005) 7670.
[24] J.P. Zhang, S.L. Zheng, X.C. Huang, X.M. Chen, Angew. Chem. Int. Ed. 43 (2004) 206.
[25] D. Li, T. Wu, X.P. Zhou, R. Zhou, X.C. Huang, Angew. Chem. Int. Ed. 44 (2005) 4175.
[26] T.B. Lu, X.M. Zhang, Y.W. Li, S. Chen, J. Am. Chem. Soc. 126 (2004) 4760.
[27] S. Hu, J.C. Chen, M.L. Tong, B. Wang, Y.X. Yan, S.R. Batten, Angew. Chem. Int. Ed. 44 (2005) 5471.
[28] Z.B. Han, Y.K. He, C.H. Ge, L. Xu, Dalton Trans. (2007) 3020.
[29] Y.K. He, Z.B. Han, Y. Ma, X.D. Zhang, Inorg. Chem. Commun. 10 (2007) 829.
[30] SHELXTL 6.10, Bruker Analytical Instrumentation, Madison, Wisconsin, USA, 2000.
[31] Z.B. Han, Y.K. He, M.L. Tong, Y.J. Song, X.M. Song, L.G. Yang, Cryst. Eng. Comm. (2008) 1070.
[32] Y.J. Song, Z.B. Han, Y.K. He, P. Zhang, J. Chem. Crystallogr. 38 (2008) 891.
[33] A.M.C.T. PLATON, Utrecht University, Utrecht, The Netherlands, Spek, A.L. 1998.
[34] N.E. Brese, M. O'Keeffe, Acta Crystallogr. Sect. B 47 (1991) 192.
[35] M.H. O'Leary, Acc. Chem. Res. 21 (1988) 450.
[36] W.G. Dauben, P. Coad, J. Am. Chem. Soc. 71 (1949) 2928.
[37] Y.J. Song, P.C. Zhao, P. Zhang, Z.B. Han, Z. Anorg. Allg. Chem. 635 (2009) 1454.
[38] P. Mahata, M. Prabu, S. Natarajan, Inorg. Chem. 47 (2008) 8451.
[39] Z.L. Lü, W. Chen, J.Q. Xu, L.J. Zhang, C.L. Pan, T.G. Wang, Inorg. Chem. Commun. 6 (2003) 244.
[40] R. Łyszczek, L. Mazur, Z. Rzączyńska, Inorg. Chem. Commun. 11 (2008) 1091.
[41] Y.Z. Zheng, M.L. Tong, X.M. Chen, N. J. Chem. 28 (2004) 1412.
[42] Y.K. He, H.Y. An, Z.B. Han, Solid State Sci. 11 (2009) 49.
[43] Z.B. Han, X.F. Li, X.N. Cheng, X.M. Chen, Z. Anorg. Allg. Chem. 631 (2005) 937.
[44] Y. Ma, Z.B. Han, Y.K. He, L.G. Yang, Chem. Commun. (2007) 4107.
[45] L. Wang, M. Yang, G.H. Li, Z. Shi, S.H. Feng, Inorg. Chem. 45 (2006) 2474.
[46] W. Chen, J.Y. Wang, C. Chen, Q. Yue, H.M. Yuan, J.S. Chen, S.N. Wang, Inorg. Chem. 42 (2003) 944.